Technical Notes

TECHNICAL NOTES are short manuscripts describing new developments or important results of a preliminary nature. These Notes cannot exceed 6 manuscript pages and 3 figures; a page of text may be substituted for a figure and vice versa. After informal review by the editors, they may be published within a few months of the date of receipt. Style requirements are the same as for regular contributions (see inside back cover).

Numerical Instabilities in the Calculation of Laminar Separation Bubbles and Their Implications

Tuncer Cebeci*
Douglas Aircraft Company, Long Beach, California

Introduction

THE laminar boundary layer on an airfoil grows from the stagnation point with a favorable pressure gradient that causes the flow to accelerate and is then subjected to an adverse pressure gradient that can cause separation with subsequent reattachment. The resulting bubbles are common on thin airfoils where the adverse pressure gradient can be sufficiently strong to cause the flow to separate even at small angles of attack and are important because of their association with the phenomenon of stall. The nature of the phenomenon is known to depend on the Reynolds number based on the radius of the leading edge and, as will be shown, the length of the separation bubble can grow to influence the location of transition. On occasions, transition can occur within the bubble. The angle of attack also is known to be important and can cause the separated region to grow until, at some angle of attack, the bubble bursts and stall sets in. This sequence of events from the first appearance of separation on the upper surface to stall is complex and requires clearer understanding than is currently available.

The prediction of separation bubbles on airfoils has been studied by a number of investigators. An important contribution was made by Briley and McDonald,[1] who used an interactive boundary-layer approach and solutions of the Navier-Stokes equations to examine the case of a comparatively thick airfoil where the separation region occurred around midchord and was approximately 10% chord in extent. Several authors[2-5] have tackled essentially the same problem with interactive boundary-layer theory. In all cases, the location of transition was either assumed to correspond to laminar separation or was computed by an empirical formula. The work of Cebeci and Schimke[4] also examined the influence of the location of transition and showed that reattachment and transition were related. Attempts to perform calculations with the experimentally reported transition location, which occurred further downstream than those considered above, revealed a tendency for the reattachment location to move rapidly downstream with the number of sweeps used in the interactive procedure. This numerical feature and its implications are examined further in this Note, together with its relationship to the location of transition.

The present approach can be described in two parts. First, we will make use of linear stability theory and the e^n method to predict transition based on calculated velocity profiles. The validity of this procedure has been demonstrated by Cebeci and Egan,[6] and calculations are presented to confirm that it is appropriate for the particular flows under investigation here. Second, we follow the approach of Ref. 7 and examine the leading-edge separation bubble on a thin airfoil as a function of angle of attack and for a Reynolds number of 10^5. This systematic study has been arranged to allow us to examine carefully the relationship between the growth of the separated region and transition.

Calculation of Transition

In a recent study, Cebeci and Egan[6] performed calculations of steady flows over and downstream of bumps identical to those examined experimentally by Fage.[8] The calculation method was based on that of Ref. 7 and solved the boundary-layer equations in an inverse mode to compute the boundary-layer characteristics including the velocity profiles and wall shear stress parameter $f''_w = (\tau_w/\rho)/u_0^2\sqrt{(u_0x/\nu)}$ for the conditions investigated by Fage. A sample of the results, in terms of f''_w, are included in Fig. 1 for a Reynolds number of 4.375×10^5 per foot and for three bump heights. Here, the Reynolds number per foot is defined in terms of the measured freestream velocity u_{1c} at the position of the centerline of the bump, but for the undistorted surface. The figure shows that the wall shear parameter decreases immediately prior to the bump, rises rapidly with the favorable pressure gradient imposed by the upstream surface of the bump, reaches a maximum, and decays rapidly to a minimum value before stabilizing as the influence of the bump diminishes. The influence of the bump height is to increase the magnitude of the maxima and minima of the f''_w distribution with a corresponding increase in its gradient.

Figure 1 also shows measured and calculated locations of transition with the latter obtained from the e^n method and the calculated velocity profiles. This method stems from the work

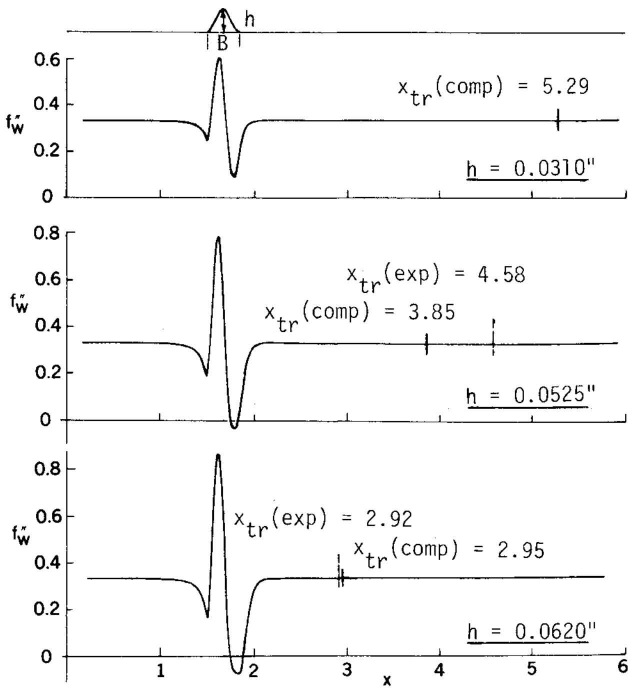

Fig. 1 Variation of wall shear parameter f''_w in the bump flows of Fage for constant Reynolds number.

Received Nov. 16, 1987; revision received April 12, 1988.

*Staff Director. Fellow AIAA.

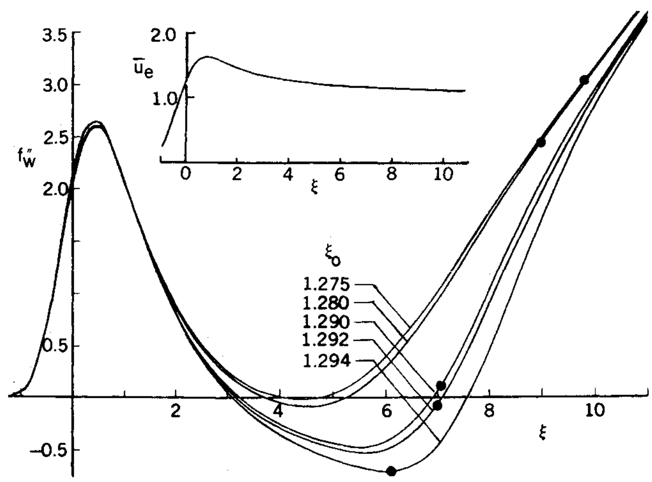

Fig. 2 Variation of external velocity distribution for $\xi_0 = 1.280$ and wall shear parameter f''_w and transition location (·) with ξ for various reduced angles of attack ξ_0 for $R = 10^5$.

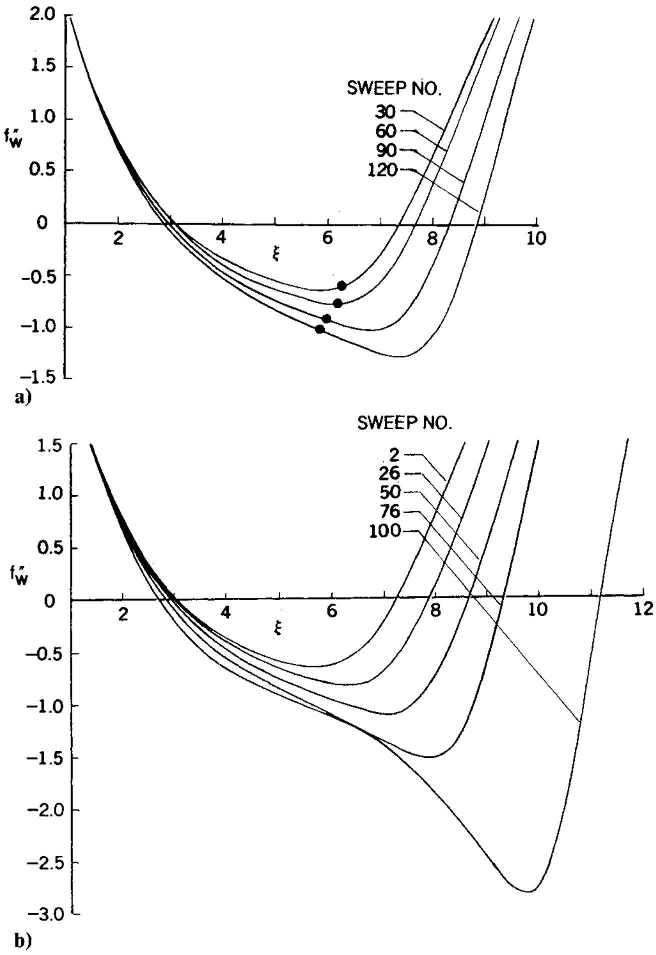

Fig. 3 Variation of a) f''_w and transition location (·) with number of sweeps for $\xi_0 = 1.296$ and b) f''_w with number of sweeps for $\xi_0 = 1.298$, $R = 10^5$.

of Refs. 9 and 10 and is based on linear stability theory. It assumes that transition starts when a small disturbance is introduced at a critical Reynolds number and is amplified by a factor of e^n. For given velocity profiles, the Orr-Sommerfeld equation is solved and stability properties are examined. The amplification rates $(-\alpha_i)$ are computed as a function of x for a range of discrete values of the frequency ω, and transition is assumed to occur when $e^{-\int \alpha_i \, dx}$ reaches a value equal to e^n, where n is around 9. In the present case, the profiles were available from the interactive boundary-layer calculations and the same version of the box scheme was used to solve the stability equation with a continuation method to obtain the eigenvalues in regions of rapidly changing f''_w and in regions of separated flow.

The agreement between measured and calculated transition locations is shown in Fig. 1 to be within experimental uncertainty; similar results were reported in Ref. 6 for the much wider range of configurations and Reynolds numbers investigated by Fage. It is clear that the location of transition moves upstream wtih increasing bump height and that the length of the separated region increases. These two characteristics also are to be found in the f''_w distributions associated with the leading-edge region of thin airfoils as discussed in the next section.

Separation Bubbles on Thin Airfoils

Following the approach of Ref. 7, we consider a thin ellipse with a thickness ratio of t at a reduced angle of attack ξ_0 in a uniform stream of velocity u_∞. In this case, the external velocity distribution is given by

$$\bar{u}_e = \frac{u_e}{u_\infty(1+t)} = \frac{\xi + \xi_0}{\sqrt{1+\xi^2}} \tag{1}$$

Here, the parameter ξ is a dimensionless distance from the nose related to the x and y coordinates of the ellipse by $x + a = \frac{1}{2}\, at^2\xi^2$ and $y = at^2\xi$ and is related to the surface distance s by

$$s = at^2 \int_0^{\xi} (1 + \xi^2)^{1/2} \, d\xi$$

The investigation of Ref. 7 made use of Eq. (1) and showed that the laminar boundary layer near the leading edge was well behaved and unseparated if $\xi_0 < \xi_s = 1.16$, although there was significant adverse pressure gradient. At higher values of ξ_0, however, separation occurred and required the use of an interactive theory to link the viscous and inviscid flows. With this theory, solutions were obtained for separation bubbles at $R(\equiv 2u_\infty a/\nu) = 2 \times 10^6$ and for $t = 0.1$, but reattachment occurred in a very limited range of the reduced angle of attack. For $\xi_0 > 1.218$, calculations broke down shortly after the flow reversal in the boundary layer and the subsequent studies of Ref. 11 led them to suggest that a dramatic switch to another separated form of motion can occur.

Figure 2 shows the f''_w distributions for several values of reduced angle of attack ξ_0 with the insert corresponding to the external velocity distribution for $\xi_0 = 1.280$. The result is similar to previous distributions reported in Ref. 6 but is presented here for a Reynolds number of 10^5, which ensures that transition occurs downstream of the separation bubble. The form of the f''_w curves resembles that of Fig. 1, particularly downstream of the beginning of the favorable pressure gradient. The wall shear stress distributions of Figs. 2 and 3 show that the region of separated flow increases in extent with ξ_0, as in Ref. 7, and expands slowly with each iteration at $\xi_0 = 1.296$ (Fig. 3a) and more rapidly at $\xi_0 = 1.298$ (Fig. 3b). This numerical instability is similar to that encountered with the bump flows of the previous section and implies that laminar flow will undergo transition before reattachment for larger bumps. This implication can be tested with the help of the stability theory described in the previous section.

The application of the e^n method to the leading-edge flows of Figs. 2 and 3 led to transition locations identified in both figures. Those in Fig. 2 exhibit the same trend noted in connection with Fig. 1 in that transition moves forward with increasing reduced angle ξ_0, which is analogous to bump height h. It is of particular note that, as ξ_0 tends to the value of 1.296 for which instability has been observed, the transition location moves toward inside the separation bubble at $\xi_0 = 1.292$. With further increase in the reduced angle of attack, the transition location moves further inside the separation bubble. At $\xi_0 = 1.296$ (see Fig. 3a), the transition location moves upstream with each sweep. These results imply that the real flow is turbulent and has a shorter recirculation region, which is consistent with experiments. It also suggests that there is little merit in expending effort to calculate the large laminar separation bubbles that would be obtained with larger reduced angles. This observation is likely to be independent of the use of interactive boundary layer or Navier-Stokes procedures.

Acknowledgment

This work was supported by the Air Force Office of Scientific Research under Contract F49620-84-C-0007.

References

[1]Briley, W. R. and McDonald, H., "Numerical Prediction of Incompressible Separation Bubbles," *Journal of Fluid Mechanics,* Vol. 69, Pt. 4, 1975, pp. 631–656.

[2]Crimi, P. and Reeves, B. L., "Analysis of Leading-Edge Separation Bubbles on Airfoils," *AIAA Journal,* Vol. 14, No. 11, March 1976, pp. 1548–1555.

[3]Kwon, O. K. and Pletcher, R. H., "Prediction of Incompressible Separated Boundary Layers Including Viscous-Inviscid Interaction," *Transactions of ASME, Journal of Fluids Engineering,* Vol. 101, No. 4, Dec. 1979, pp. 466–472.

[4]Cebeci, T. and Schimke, S. M., "The Calculation of Separation Bubbles in Interactive Turbulent Boundary Layers," *Journal of Fluid Mechanics,* Vol. 131, June 1983, pp. 305–317.

[5]Carter, J. E. and Vatsa, V. N., "Analysis of Airfoil Leading-Edge Separation Bubbles," NACA CR 165935, May 1982.

[6]Cebeci, T. and Egan, D. A., "The Effect of Wave-Like Roughness on Transition," AIAA Paper 88-0139, Jan. 1988.

[7]Cebeci, T., Stewartson, K., and Williams, P. G., "Separation and Reattachment Near the Leading Edge of a Thin Airfoil at Incidence," AGARD CP-291, 1981.

[8]Fage, A., "The Smallest Size of a Spanwise Surface Corrugation Which Affects Boundary-Layer Transition on an Aerofoil," British Aeronautical Research Council, London, R&M 2120, 1943.

[9]Smith, A. M. O. and Gamberoni, N., "Transition, Pressure Gradient and Stability Theory," *Proceedings of the Ninth International Congress on Applied Mechanics,* Brussels, 1956, Vol. 4, pp. 234–244.

[10]Van Ingen, J. L., "A Suggested Semi-Empirical Method for the Calculation of the Boundary-Layer Region," V.T.H., Delft, the Netherlands, Rept. VTH 71, 1956.

[11]Stewartson, K., Smith, F. T., and Kaups, K., "Marginal Separation," *Studies in Applied Mathematics,* Vol. 67, Aug. 1982, pp. 45–61.

Analysis of Multi-Element Airfoils by a Vortex Panel Method

H. N. V. Dutt*

National Aeronautical Laboratory, Bangalore, India

Nomenclature

$A_{i,j}$ = influence coefficient matrix
b_i = right-hand side of Eq. (2) (function of σ)
C_p = pressure coefficients
C = multi-element airfoil contour
F = function entering the Cauchy-type integral, Eq. (1)
f = jump of F across airfoil contour
$m(l)$ = number of points on lth component
N = number of points defining multi-element system
N_c = number of components
u = tangential component of velocity
v = normal component of velocity
(x,y) = coordinate of airfoil
Z = complex position vector
α = angle of attack
γ = vortex strength
σ = source strength
ϕ = angle between exterior normal to C and real axis
θ = trailing-edge angle

Subscripts

i,j = panel indices
L = lower surface
U = upper surface

Received July 30, 1987.

*Scientist, Aerodynamics Division.

Introduction

SEVERAL methods exist for the analysis of single or multi-element airfoils in potential flows.[1–7] Most of these methods have one or more of the following drawbacks: use of multiple singularities either to alleviate the problem of pressure oscillations near trailing edges of thin airfoils, or to represent the thickness and lifting effects for finite-thickness lifting airfoils;[1–4] use of panel method in a mapped plane when trailing edge is cusped;[5] need to represent airfoil by large number of points to get acceptable results.[6] Also, most of the methods output the pressure coefficients at panel midpoints, which in fact are not the points on the given contour.

In the present Note, we describe a "vortex alone" formulation for the analysis of multi-element airfoils, which does not suffer from any of the problems listed above. Versatility of this formulation is demonstrated by analyzing thin or cusped airfoils and airfoils with two, three, or four elements for which exact results are available.

Method of Analysis

Let $Z = x + iy$ be the complex position vector in the airfoil plane (Fig. 1). Identifying $F(Z)$ with the complex disturbance velocity in the Cauchy-type of integral

$$F(Z) = \frac{1}{2\pi i} \int \frac{f(Z')}{Z' - Z} \, \mathrm{d}Z' \tag{1}$$

where $f(Z')$ is jump of function F across the contour C, by writing

$$f(Z') = -[\sigma(Z') + i\gamma(Z')]e^{-i\phi(Z')}$$

it can be shown that the normal and tangential components are given by

$$v(Z) = \mathrm{Re}\,\{[e^{-i\alpha} + F^-(Z)]e^{i\phi(z)}\} = \sigma(Z)$$

$$u(Z) = -\mathrm{Im}\,\{[e^{-i\alpha} + F^-(Z)]e^{i\phi(z)}\} = -\gamma(Z)$$

respectively, where α is freestream incidence. Here, nonzero values of σ can be used to simulate the displacement effects of the boundary layer. Zero value of σ implies tangential inviscid flow and leads to a vortex alone formulation for the potential flow over multi-element airfoils. The trailing-edge Kutta con-

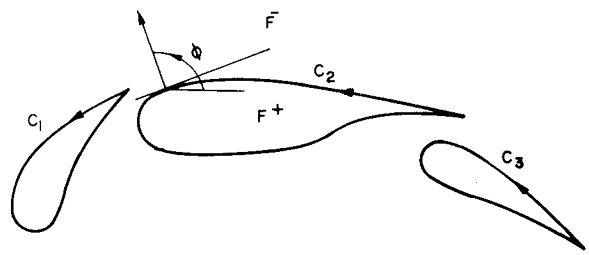

Fig. 1 Complex Z-plane.